American Journal of Biochemistry and Biotechnology

Research Article

Optimization of α-Glucosidase Inhibitors Recovery from Rainbow Trout Hydrolysate Using GA-BP Neural Network

Yingke Chu[1], Yanling Dong[2], Qingfeng Rong[2], Kun Yang[2] and Lanlan Zhu[1]

[1]*College of Agricultural Engineering and Food Science, Shandong University of Technology, Zibo, 255100, Shandong Province, China*
[2]*Test Center, Zichuan District Inspection and Test Center, Zibo, 255100, Shandong Province, China*

Article history
Received: 01-10-2024
Revised: 17-12-2024
Accepted: 18-01-2025

Corresponding Author:
Lanlan Zhu
College of Agricultural Engineering and Food Science, Shandong University of Technology, Zibo, 255100, Shandong Province, China
Email: chinaxiaolan@163.com

Abstract: To enhance the value of by-products from rainbow trout processing, the inhibition rate of α-glucosidase (AGIR) is used as indicators. Optimization of rainbow trout hydrolysate extraction by comparing Response Surface Methodology (RSM) and BP Neural Network (BPNN) models. The RSM results: the AGIR is 55.02%. BPNN models predicted the optimal extraction conditions: 51 °C for temperature,1:2.3 for solid-liquid ratio, 4.15 h for time and 0.2334% for enzyme dosage. The reactions obtained under optimized conditions are as follows: the α-glucosidase inhibitory rate increased to 58.14%. This proves that the BPNN model can simultaneously improve the hydrolysis degree and α-glucosidase inhibition rate of the rainbow trout hydrolysate.

Keywords: Rainbow Trout, Enzymatic Hydrolysis Reaction, BP Neural Network

Introduction

Diabetes is a metabolic syndrome characterized by impaired insulin secretion and action, leading to a range of clinical manifestations, including hypertension (Khan *et al.*, 2019; Fatumo, 2024). A key therapeutic target for managing type II diabetes is the enzyme α-glucosidase (Kumari *et al.*, 2024). However, due to adverse effects such as hypersensitivity and hepatotoxicity associated with current α-glucosidase inhibitors, research continues to seek novel, safer alternatives (Alam *et al.*, 2019).

Rainbow trout is a globally cultivated species in aquaculture. Its flesh is rich in bioactive peptides (Nguyen *et al.*, 2022; Refstie *et al.*, 2000) and hydrolysates derived from rainbow trout have demonstrated significant biological effects, including antioxidant, anti-inflammatory, and pronounced α-glucosidase inhibitory activity (Bartolomei *et al.*, 2023). As α-glucosidase is a key therapeutic target for diabetes management, these findings are particularly relevant. Rainbow trout skin, a major processing by-product with currently low commercial value, represents a promising source for these bioactive peptides. Therefore, this study aimed to optimize the extraction of peptides from rainbow trout skin and assess their in vitro α-glucosidase inhibitory activity, with a view to developing a potential high-value product for the food industry.

Bioactive peptides are increasingly being extracted from marine sources worldwide (Bleakley & Hayes, 2017; Lemes *et al.*, 2016). Rainbow trout, rich in protein and hydrophobic amino acids, is a promising substrate for generating such peptides (Zhou *et al.*, 2024). Its skin, a major by-product of fillet processing with minimal commercial value, is often discarded as waste (Wang *et al.*, 2008). However, this protein-rich material holds significant potential for valorization in food products (de Andrade Silva *et al.*, 2020).

The enzymatic hydrolysis process used to extract these peptides is complex. Outcomes vary based on protease type and activity, which influence cleavage sites, hydrolysis degree, final bioactivity, and peptide sequences (Morales-Medina *et al.*, 2016). Critical parameters, including reaction time, solid-liquid ratio, temperature, and enzyme dosage, further affect the process (Coscueta *et al.*, 2021; Martinez-Araiza *et al.*, 2012).

Traditional optimization using Response Surface Methodology (RSM) is limited by its quadratic framework and sensitivity to non-fitting variables (Kuo *et al.*, 2014). While Backpropagation Neural Networks (BPNN) effectively model the nonlinear relationships in enzymatic hydrolysis (Zheng *et al.*, 2013), existing applications have focused on single objectives (e.g., degree of hydrolysis). A comprehensive framework that simultaneously optimizes for multiple targets, such as hydrolysis efficiency, bioactive yield, and sensory quality, is lacking. Furthermore, the dynamic, nonlinear coupling of process parameters remains underexplored, hindering real-time adaptive control.

DOI: 10.3844/ajbbsp.2025.401.411

This study addresses these gaps by integrating a Genetic Algorithm (GA) for global search with a BPNN for local gradient optimization (Ermias, 2021). We introduce parameter sensitivity analysis to guide an adaptive weight adjustment algorithm, improving model training and convergence speed. A multi-objective optimization framework is established by incorporating two key indicators, degree of hydrolysis and α-glucosidase inhibition rate, into the BPNN. Their contributions are balanced using the entropy weight method for dynamic weight allocation (Piyush *et al.*, 2021; Mehta *et al.*, 2022; Hang *et al.*, 2021).

Previous studies have primarily focused on the effects of enzymatic hydrolysis on peptides, but there is limited literature on the optimization of enzymatic hydrolysis for recovering α-glucosidase inhibitors using GA-BP Neural Networks. This study conducted single-factor experiments to investigate the impact of papain protease dosage, solid-liquid ratio, reaction time, and temperature on the yield of rainbow trout peptides. Subsequently, the study utilized BPNN to optimize the extraction process of rainbow trout peptides and examined their inhibitory activity against α-glucosidase. By optimizing the extraction process and delving into the activity of rainbow trout peptides, this research provides a reference for developing novel, high-value products from rainbow trout for comprehensive utilization.

Materials and Methods

Materials

Rainbow trout (with a composition of 7.33% moisture, 18.82% protein, 3.64% crude fat, and 1.06% ash) was supplied by the Boshan Qinglongtan Aquaculture Farm. Papain (>200 U·mg and α-glucosidase (Shanghai Yuanye Biotechnology Co., Ltd..); PNPG (4-nitrophenyl-β-D-pyranoside, Shanghai Yuan Ye Biotechnology Co., Ltd.) were used in the study. Acetonitrile and trifluoroacetic acid were of chromatographic grade, while other reagents were of analytical grade. Equipment utilized included the GB204 electronic balance (Mettler-Toledo, Switzerland); THZ-82 constant temperature oscillating water bath (Jingda Instrument Manufacturing Factory, TianJin City); 3K30 benchtop high-speed refrigerated centrifuge (Sigma, Germany); Alpha1-4 vacuum freeze dryer (Christ, Germany); and Sunrise-basic Tacan SUNRISE microplate reader (TECAN, Switzerland).

Extraction

The rainbow trout skin was pulverized into a powder using a grinder, and then distilled water was added in a specific ratio to facilitate crushing. Papain protease was added at different reaction temperature and time. Following the completion of hydrolysis, the enzyme was deactivated by immersing the solution in boiling water for 15 minutes, cooled to room temperature, and centrifuged at 10000 r/min for 20 minutes. The supernatant was collected and freeze-dried to obtain the rainbow trout skin enzymatic hydrolysate freeze-dried powder.

Determination of α-Glucosidase Inhibition Rate of Rainbow Trout Skin Extract

α-glucosidase inhibition rate was assessed using a UV-Vis spectrophotometric method, which involved the enzymatic reaction with PNPG substrate solution. slight modifications were made to prepare solutions of α-glucosidase and PNPG at concentrations of 0.25 U·mL and 2 mmol·L, respectively, in a phosphate buffer saline (PBS) solution with a pH of 6.8 and a concentration of 100 mmol·L. A 100 μL sample solution and 50 μL of α-glucosidase solution were transferred to a 96-well enzyme plate, mixed, and then incubated at 37°C for 15 minutes. Subsequently, 50 μL of PNPG solution was added, and the reaction was allowed to proceed at 37°C for 20 minutes. Finally, 100 μL of sodium carbonate (NaCO) solution at a concentration of 200 mmol·L was added to terminate the reaction. The absorbance value (As) was measured at a wavelength of 405 nm using a spectrophotometer. The absorbance of the buffer solution (Ac) was measured in place of the sample solution, and the absorbance of PBS was measured in place of α-glucosidase to obtain the absorbance value (An). The inhibition rate of α-glucosid：

$$R_{\mathrm{a}} = \frac{A_{\mathrm{c}} - (A_{\mathrm{s}} - A_{\mathrm{n}})}{A_{\mathrm{c}}} \times 100\%$$

Design of Experiments

The effects of four independent variables: reaction temperature (X1), reaction time (X2), enzyme dosage (X3) and solid-liquid ratio (X4) on two dependent variables: α-glucosidase inhibition rate (Y1) and hydrolysis degree (Y2) were initially examined using the One-Factor-At-a-Time approach to establish the appropriate ranges for the input parameters.

Single-Factor Experiment

Papain was selected as the enzymatic protease for the enzymatic hydrolysis of rainbow trout by-products. A single factor experiment was conducted with α-glucosidase inhibition rate and hydrolysis degree as screening indicators. The experimental levels are selected as reaction time of 1.5 h, 2.5 h, 3.5 h, 4.5 h, 5.5 h, and 6.5 h; reaction temperature of 40.0 °C, 45.0 °C, 50.0°C, 55.0°C, 60.0°C, and 65.0°C; enzyme addition of 0.1%, 0.2%, 0.3%, 0.4%, and 0.5%; and solid-liquid ratio of 1:1, 1:2, 1:3, 1:4, and 1:5. The enzymatic hydrolysis conditions are preliminarily optimized to determine the optimal factor test parameters. Each treatment was repeated 3 times, and the results are averaged.

Response Design

Utilizing the framework of the Box-Behnken experimental design, a four-factor, three-level study was

DOI: 10.3844/ajbbsp.2025.401.411

performed, wherein the α-glucosidase inhibition rate (Y1) and hydrolysis rate (Y2) served as the response variables. The factors investigated included enzyme reaction time (A), enzyme addition amount (B), reaction temperature (C), and solid-to-liquid ratio (D). Table 1 details the factor levels for the experimental design, which were determined through preliminary single-factor experiments.

Table 1: Levels of response surface test

Level	Factor			
	A:Enzymolysis time/h	B:Enzyme dosage/%	C:Enzymolysis temperature/°C	D:Material-liquid ratio
-1	2.5	0.1	45	1:1
0	4.5	0.2	50	1:2
1	6.5	0.3	55	1:3

Neural Network and Genetic Algorithm Optimization Process

BPNN Modeling

The Backpropagation Neural Network (BPNN), as a fundamental type of neural network, is extensively utilized in various applications. BPNN is composed of numerous nodes organized into three distinct categories of layers: the input layer, one or more hidden layers, and the output layer. The input and output layers correspond to the elements and corresponding reactions, respectively. The signal is modified by the activation function as it progresses from the input layer to the output layer, passing through the intermediate hidden nodes. Upon completion of the training process, a correlation between the variables and the corresponding outcomes is determined. In this research, the input layer of the BPNN comprises four neurons, each corresponding to specific parameters: reaction temperature, reaction time, solid-liquid ratio, and the quantity of enzyme added. Conversely, the output layer of the BPNN consists of two neurons, which denote the α-glucosidase inhibition rate and the degree of hydrolysis. The determination of the optimal number of neurons within the hidden layer is intricately linked to the prediction results of the model. The quantity of neurons within the hidden layer can be determined utilizing equation (1.1). The evaluation of the quality of the developed models was performed through the application of analysis of variance (ANOVA), which involved the evaluation of the coefficient of determination (R^2), the predicted coefficient of determination (R^2-predicted), as well as the calculation of percentage errors and the root mean square error (RMSE) in relation to the predicted and observed values.

$$h=\sqrt{m+n}+z$$

Where, h is the number of neurons in the hidden layer, m represents the quantity of nodes within the input layer, while n denotes the quantity of nodes in the output layer, z is a tuning constant between 1 and 10 ($1\leq z\leq 10$).

Sample Selection and Training

The models that guaranteed quality are utilized to identify the best conditions for the procedure of extraction. In pursuit of maximizing the AGIR and achieving the highest degree of hydrolysis, the desirability function methodology was employed to identify the optimal values of the independent variables. The validation assessment was conducted in triplicate under specified ideal conditions, and the α-glucosidase inhibition rate and degree of hydrolysis (n) are compared with the predicted values.

This function operates on responses within the range of [0,1]. The output layer, which consists of two neurons, integrates the responses received from the hidden layer. This response is ultimately analyzed through the application pertaining to a novel transfer function. In this context, three distinct transfer functions are evaluated: “Tansig” “Purelin” “Trainlm”.

The 81 sets of input data are divided into three subsets, with the first subset containing 70% of the experimental data, which is used for training the neural network. Training involves the process of identifying the optimal weight vector and biases that align the generated responses with the corresponding independent variables. The LM, as implemented in MATLAB 2019a, was selected to iteratively adjust the weights and bias in order to minimize the MSE between the observed and predicted output variables. A total of 30 training sessions were conducted for each specified quantity of neurons within the hidden layer, ranging from 1 to 10, to ensure a sufficient representation of the data. In each individual training session, the maximum number of iterations, or epochs, was constrained to 10000. The validation subset constituted 15% of the experimental data. During the iterative process, the errors associated with this subset are tracked and utilized as a criterion for implementing early stopping. In this methodology, the training process was halted upon observing a rise in the validation subset error for a duration of 10 consecutive iterations. This mitigates the risk of overfitting, a phenomenon characterized by a decline in predictive performance resulting from the overtraining of the network. The remaining 15% of the experimental dataset is analyzed separately to calculate the test error.

Genetic Algorithms for Optimal Inheritance

GA demonstrates proficiency in global search, while the BPNN exhibits greater efficacy in local search. Consequently, the integration of the GA with the BP algorithm proves to be highly effective. The objective of

employing GA to enhance BPNN is to obtain more suitable initial weights and thresholds for the network through genetic optimization techniques. The GA is a global multipoint search technique employed to address optimization problems. It utilizes probabilistic transfer rules to facilitate the search process. Considering each feature as a genetic individual, the prediction error of the initialized BPNN is used as the fitness value for the individual, and the optimal individual, the optimal initial parameters and thresholds of the BPNN, is searched for through selection, crossover, and mutation , and then the actual values of the corresponding parameters are decoded. When setting the initial parameters of the GA, the crossover probability and the mutation probability generally take values between 0 and 1. In this study, the maximum value of evolutionary generations is established at 50, the population size is set to be 30, the crossover probability is determined to be 0.75, and the mutation probability is set at 0.21.

Statistical Analysis

Design Expert.V8.0.6 and Origin 2022 software are used for experimental design and data analysis, and MATLAB 2019a software was used for neural network construction and training.

Results and Discussion

Single-Factor Experiment Results

Effect of Enzyme Addition on System

As illustrated in Fig. 1, the AGIR initially increased and then decreased as the amount of enzyme added increased. The AGIR rose with enzyme addition from 0.1% to 0.2%, reaching a maximum value (38.94%) at 0.2% enzyme addition; the inhibition rate decreased significantly when enzyme addition exceeded 0.2% ($P < 0.05$). Under identical conditions, increasing protease dosage accelerates substrate protein decomposition, producing more small-molecule peptides or free amino acids, thereby enhancing the inhibitory activity of enzyme digests against α-glucosidase (Wu *et al.*, 2019). Li-na *et al.* (2018) prepared α-glucosidase inhibitory peptides from peanut proteins using alkaline protease and found that AGIR increased with enzyme addition up to 1.2%, then declined when exceeding this level. However, excessive enzyme addition can cause further degradation of polypeptides with strong inhibitory activity, altering amino acid composition and sequence, and thus reducing inhibition. Therefore, 0.2% enzyme addition was selected as the optimal level for further optimization.

Influence of Solid-Liquid Ratio on Enzymatic Reaction System

As shown in Fig. 2, when the solid–liquid ratio is 1:2, the α-glucosidase inhibitory activity of the digest reaches its highest value, with an inhibition rate of 52.18%. At ratios of 1:1, 1:3, 1:4, and 1:5, the inhibitory activity significantly decreases ($P < 0.05$). When the solid–liquid ratio is 1:1, the enzyme's diffusion movement is limited, preventing sufficient binding to the substrate and thus hindering the enzymatic reaction, which reduces the inhibitory activity of the digest product on α-glucosidase (Mora & Toldrá, 2023). Although higher solid–liquid ratios reduce the viscosity and allow adequate enzyme–substrate interaction, the lower substrate concentration slows the enzymatic digestion under the same conditions. A similar observation was made by O'Meara & Munro (1984) who used pepsin to generate ACE inhibitory peptides from soybean protein; when the solid–liquid ratio was below 1:2, the AGIR increased with enzyme amount, but declined once the ratio exceeded 1:2 (Mazorra-Manzano *et al.*, 2017). Therefore, the optimal solid–liquid ratio for enzymatic digestion was determined to be 1:2.

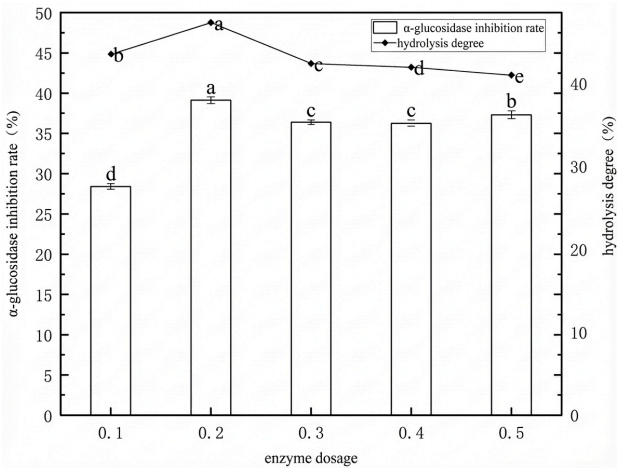

Fig. 1: Effect of enzyme on enzymatic reaction system

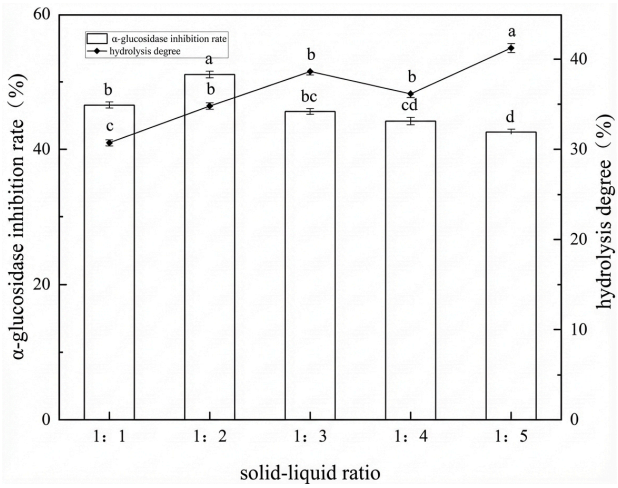

Fig. 2: Effect of different solid–liquid ratios on α-glucosidase inhibitory activity

Effect of Reaction Time on the System

As illustrated in Fig. 3, the AGIR showed an increasing trend as the reaction time extended from 1.5 to 4.5 hours. The AGIR reached its maximum value

(42.63%) at 4.5 hours and then gradually declined with further prolongation of enzymatic digestion ($P < 0.05$), decreasing to 24.42% at 6.5 hours. This decline occurs because prolonged hydrolysis leads to further decomposition of peptides with high inhibitory activity, destroying active groups and reducing α-glucosidase inhibition (Mazorra-Manzano *et al.*, 2017). These findings align with those of (Meng *et al.*, 2022), who prepared α-glucosidase inhibitory peptides from Antarctic krill protein using complex protease. Their study showed that AGIR increased linearly between 4 and 6 hours, reaching a peak value of 59.39% at 6 hours, followed by a gradual decline between 6 and 8 hours. After 4.5 hours of enzymatic hydrolysis, the degree of hydrolysis (DH) was 34.95%. Therefore, 4.5 hours was selected as the optimal reaction time for further optimization of the enzymatic digestion process.

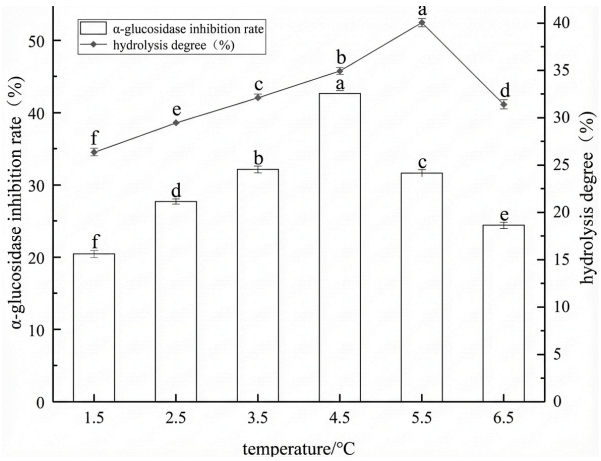

Fig. 3: Effect of reaction time on the enzymatic reaction system

Effect of Reaction Temperature on the Merad Reaction System

Temperature influences enzymatic hydrolysis by affecting enzyme activity. As shown in Fig. 4, within the range of 40–55°C, the inhibition rate gradually increased with temperature and reached its maximum value (54.56%) at 55°C. Although papain's optimal temperature is 50°C, AGIR continued to increase beyond that point, likely because the enzyme's spatial structure remained intact within this range. The elevated temperature promotes effective molecular collisions, accelerates enzymatic reactions, and exposes active groups, enhancing α-glucosidase inhibitory activity (Fernández-Lucas *et al.*, 2017). However, when the temperature exceeds acceptable limits, the spatial structure of some enzymes becomes denatured and inactivated, slowing the reaction and reducing inhibitory activity. Sánchez & Vázquez (2017) observed a similar trend when preparing α-glucosidase inhibitory peptides from *Undaria pinnatifida*, where AGIR initially increased and then declined with rising temperature. Therefore, 55 °C was selected as the optimal reaction temperature for further enzymatic digestion optimization.

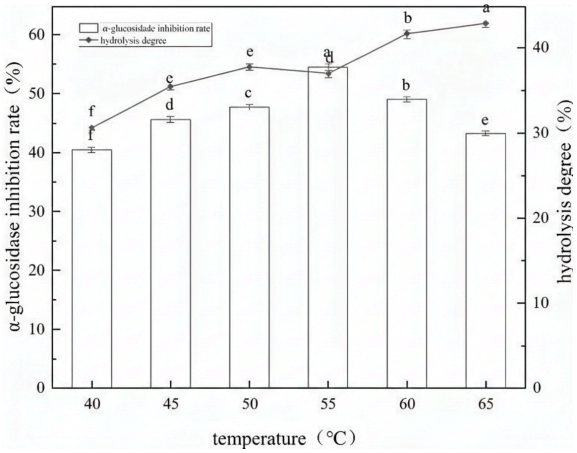

Fig. 4: Effect of reaction temperature on the enzymatic reaction system

BPNN Optimization

Results of α-Glucosidase Inhibition Rate of Rainbow Trout Enzyme Digests

On the basis of one-way test, enzyme addition amount, reaction time, reaction temperature, and solid-liquid ratio are selected and tested by Box-Behnken experimental design. The experimental results are shown in Table 2. The factors and outcomes presented in Table 3 were analyzed using multiple quadratic regression fitting with Design-Expert 130, resulting in the following model regression equation $Y = 45.377 + 15.34846A + 2.816B + 15.6544C + 464.25383D + 0.1055AB + 0.105AC - 3.07AD - 0.6125BC - 10.6894BD - 12.17069CD - 0.133775A^2 - 0.626201B^2 - 4.61583C^2 - 501.22629D^2$.

Table 3 indicates that the F for this model was 26.09, with a corresponding P of less than 0.01, thereby categorizing the model as extremely important. The p-value for the lack-of-fit was 0.2457, which exceeds the threshold of 005. This suggests that the model wasn't significantly influenced by the lack-of-fit factor. The R^2 was calculated to be 0.9631. Furthermore, the disparity between the Adjusted R^2 and the Predicted R^2 was found to be 0.1341, which is less than the threshold of 0.2. This suggests that the model sufficiently represents the actual conditions. The significance values associated with factors A, B, C, D presented in Table 3 were all below 0.05, suggesting that the Y was significantly affected by these factors. Furthermore, the significance values for factors A, B, C, D were below 0.01, The significance values for factors A, B, C, and D were all below 0.01, showing that factors had highly significant impacts on Y.

Figure 5 illustrates that the response variable Y exhibited an initial increase followed by a decrease as the levels of the factors A, B, C, and D were elevated in interactions involving two elements. The best conditions identified through the analysis were determined to be 51°C for temperature,1:2.3 for solid-liquid ratio, 4.15 h for time and 0.2334% for enzyme dosage.

Table 2: Results of Enzymatic reaction

Sample number	Enzyme dosage/%	Material-liquid ratio	Enzymolysis time/h	Enzymolysis temperature/°C	α-Glucosidase inhibition
1	0.2	1:2	6.5	60	44.41
2	0.2	1:2	6.5	50	43.48
3	0.2	1:1	6.5	55	37.26
4	0.2	1:3	6.5	55	48.10
5	0.1	1:2	6.5	55	42.03
6	0.3	1:2	6.5	55	42.70
7	0.2	1:1	4.5	50	44.47
8	0.2	1:3	4.5	50	47.12
9	0.3	1:2	4.5	50	46.45
10	0.1	1:2	4.5	50	40.38
11	0.1	1:3	4.5	55	42.56
12	0.1	1:1	4.5	55	49.27
13	0.2	1:2	4.5	55	54.87
14	0.2	1:2	4.5	55	55.21
15	0.2	1:2	4.5	55	56.33
16	0.3	1:1	4.5	55	45.66
17	0.3	1:3	4.5	55	40.52
18	0.3	1:2	4.5	60	42.04
19	0.1	1:2	4.5	60	45.13
20	0.2	1:1	4.5	60	32.69
21	0.2	1:3	4.5	60	46.35
22	0.2	1:1	2.5	55	40.94
23	0.2	1:3	2.5	55	42.77
24	0.3	1:2	2.5	55	43.48
25	0.1	1:2	2.5	55	43.21
26	0.2	1:2	2.5	60	42.17
27	0.2	1:2	2.5	50	39.63

Table 3: Evaluation of the RSM model

Source	Sum of Square	df	Mean Square	F	P	Significance
Model	633.94	14	45.28	26.09	<0.0001	**
A	152.23	1	152.23	87.72	<0.0001	**
B	9.83	1	9.83	5.66	0.0321	*
C	67.07	1	67.07	38.65	<0.0001	**
D	67.74	1	67.74	39.03	<0.0001	**
AB	5.38	1	5.38	3.10	0.1000	
AC	1.38	1	1.38	0.7956	0.3875	
AD	7.21	1	7.21	4.15	0.0609	*
BC	5.34	1	5.34	3.08	0.1014	
BD	17.14	1	17.14	9.88	0.0072	*
CD	3.57	1	3.57	2.06	0.1733	
A	152.23	1	152.23	87.72	<0.0001	**
B	9.83	1	9.83	5.66	0.0321	
C	67.07	1	67.07	38.65	<0.0001	**
D	67.74	1	67.74	39.03	<0.0001	**
Residual	24.29	14	1.74			
Lack of fit	20.42	10	2.04	2.11	0.2457	
Pure error	3.87	4	0.9679			
Cor total	658.23	28				
$R^2 = 0.9631$	Adjusted $R^2 = 0.9262$	Predicted $R^2 = 0.7921$	Std. Dev. = 1.36			

BPNN Hidden Layer Node Optimization

The BPNN modeling is carried out using MATLAB and the BPNN is trained using the test data. In the process of training the neural network using the software, 81 sets of experimental data are randomly divided into training, validation, and testing parts for the iterative training of the BPNN model in accordance with the ratio of 70%, 15% and 15%. The optimal number of hidden layer nodes was determined using a standard empirical formula. Based on this formula, a range of 2 to 13 nodes was selected for testing. Table 4 displays the MSE of the

BPNN model set up with different quantities of hidden neurons. When the number of neurons in the hidden layer is 10, the BPNN model achieved its minimum MSE of 00068 after 55 iterations, as illustrated in Figure 6.

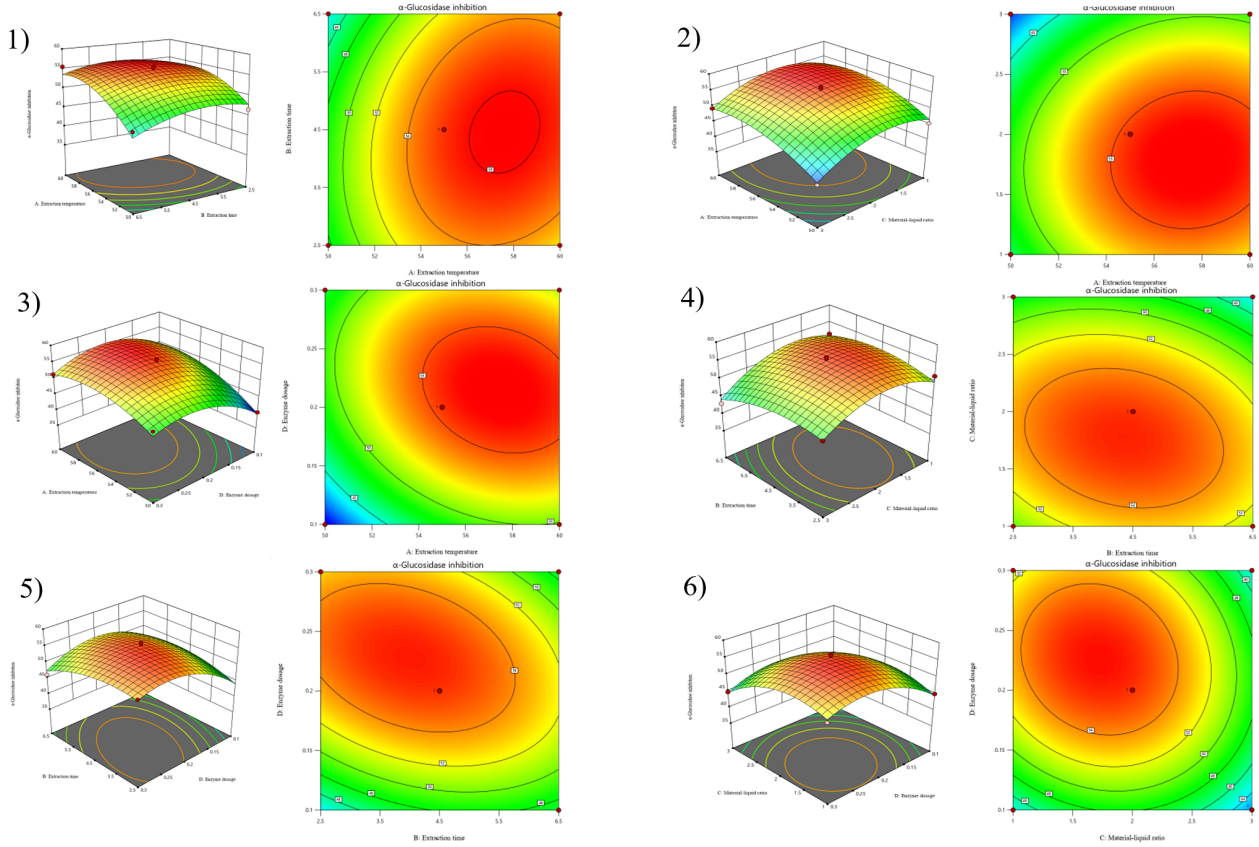

Fig. 5: The three-dimensional surface plot and contour analysis of the model

Table 4: Number of nodes in the hidden layer and MSE

Number of Nodes	Mean Square Error
2	0.0311
3	0.0493
4	0.0359
5	0.0219
6	0.0683
7	0.0146
8	0.0239
9	0.0293
10	0.0067
11	0.0145
12	0.0202
13	0.0916

BP Neural Network Modeling

The smaller the MSE value of the MSE evaluation, the higher the accuracy of the constructed neural network model in predicting the test data. The learning and training process of BPNN is shown in Figure 7. From the curve shown in the figure, it can be seen that the network training is more stable and converges rapidly, and the neural network after the enzymatic reaction reaches the set mean-square error target requirement of the network performance after 49 iterations, which indicates that the structure and parameters of BP Neural Network model established by the research are more reasonable and can be used for the fitting research of Freshening Technology. This indicates that the structure and parameters of the BP Neural Network model established in this study are reasonable and can be used for the fitting study of the Melad freshening technology.

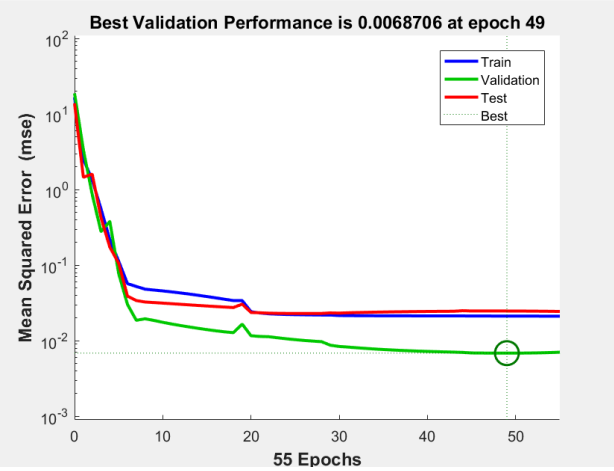

Fig. 6: Training process of BP Neural Network model for sensory scores

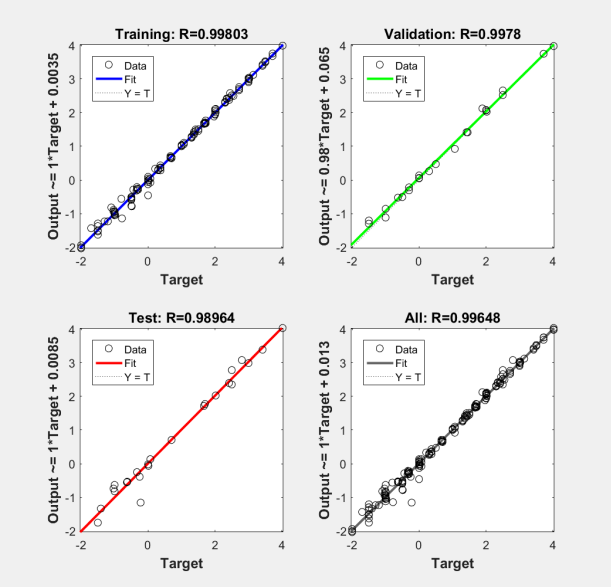

Fig. 7: BP Neural Network model correlation coefficient evaluation

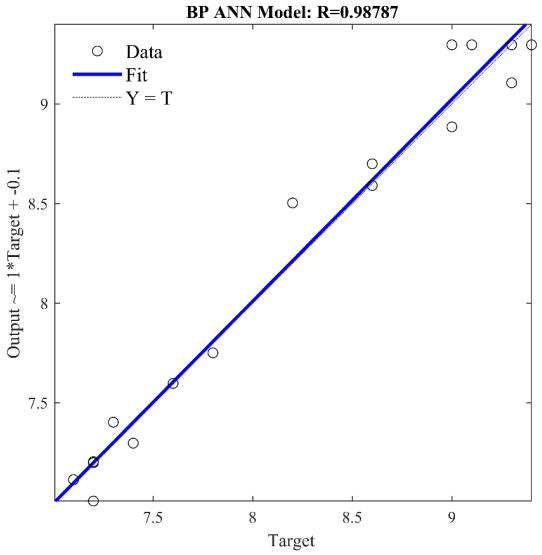

Fig. 8: Regression analysis of target and network outputs after the enzymatic reaction

Evaluation of Correlation Coefficients for BP Neural Network Models

The output values and target values for the training, validation, testing, and overall datasets have been quantified, and the associated correlation coefficients have been computed, as illustrated in Figure 7. The data presented in the figure indicates that the correlation coefficient (R) values for the training set (099803), validation set (09978), test set (098964), and the overall prediction set (099648) suggest that BPNN model has superior regression and fitting performance. In Figure 8, the majority of data points are distributed closely along the 45°line, suggesting a strong correlation between the test results and the predicted values generated by the BPNN. The target value and the output value of the neural network model exhibit a substantial positive correlation, thereby providing further evidence that the BPNN model has been effectively developed with a high degree of fitting accuracy.

BP Neural Network Model Training Accuracy Analysis

Figure 8 shows the regression straight line between the network output value Y and the network target value X for the test sample of the BPNN model. The network output value Y is the output value calculated using the trained genetic BPNN model. The network target value X is the measured value that the BPNN is trained to achieve. As illustrated in the figure, the correlation coefficient R of the regression straight line is 0.98787, which are all close to 1. In addition, the regression line basically coincides with the straight line with slope 1 (Y=X), which indicates that the output value of the BP Neural Network has very little deviation from its target value, and it is a very effective prediction method.

Genetic Algorithm Optimization and Validation Tests

The GA is utilized to identify temperature and enzyme addition amont as critical variables from four enzymatic hydrolysis parameters. BPNN Is subsequently developed to establish a nonlinear mapping relationship based on experimental datasets, which reduced the mean MSE of hydrolysis degree prediction from 0.042 in conventional univariate models to 0.006. To further enhance model performance, a parameter sensitivity analysis framework was incorporated, coupled with an adaptive weight adjustment algorithm that optimized network training dynamics. This hybrid approach achieved a 40% acceleration in convergence speed while maintaining high prediction accuracy , demonstrating superior efficiency in enzymatic hydrolysis process modeling.

Comparative Examination of RSM and BPNN Models

Analysis of Model Error Comparison

The error analysis related to RSM and BPNN is shown in Table 4. The model was assessed by calculating and comparing several statistical metrics, including the R^2, RMSE, MAD, and Spherical Probability Error (SPE).

$$R^2 = \frac{\left(\sum_{i=1}^{n}\left(Y_1-\overline{Y}_1\right)\left(Y_1-\overline{Y}_p\right)\right)^2}{\left(\sum_{i=1}^{n}\left(Y_1-\overline{Y}_1\right)\left(Y_p-\overline{Y}_p\right)\right)^2}$$

$$\text{RMSE} = \left(\frac{1}{n}\sum_{i=1}^{n}\left(Y_p - Y_1\right)^2\right)^{\frac{1}{2}}$$

$$\text{MAD}\,(\%) = \frac{1}{n}\sum_{i=1}^{n}\frac{\left|Y_1-\overline{Y}_1\right|}{|Y_1|} \times 100\%$$

$$\text{SPE}\,(\%) = \frac{\text{RSME}}{\overline{Y}_1} \times 100\%$$

n denotes the quantity of samples, Y signifies the test value, $\overline{Y1}$ indicates the mean of the test samples, Y denotes the predicted value generated by the model, and $\overline{Yp}$ refers to the mean of the model's predicted values.

Table 5: Parameter comparison of two models

Model	R	RMSE	MAD	SPE
RSM	0.94877	0.9017	4.0727	1.96
BPNN	0.99648	0.3687	4.1746	0.74

The RMSE, MAD, and SPE values were low, while the model's R was high, suggesting that the model demonstrated strong accuracy and reliability (Wu *et al.*, 2019). Table 5 demonstrates that the R^2 for the BPNN model exceeded that of the RSM. Additionally, the RMSE and SPE values for the BPNN model were lower than those of the RSM, suggesting that BPNN model outperformed the RSM in terms of predictive accuracy.

Validation of the Optimal Solutions Derived from the Models

In Table 6 the AGIR of 58.61 （mg/g） predicted by the BPNN exceeded the 56.44 （mg/g） forecasted by the RSM, while also exhibiting a lower relative error compared to the RSM model. Consequently, it can be inferred that the BPNN model demonstrated greater efficacy compared to the RSM in optimizing the extraction process. The outcome aligns with the conclusions drawn by Li-na *et al.* (2018).

Table 6: Comparison and Validation of the Models

Model	time/h	Temperature/°C	solid-liquid ratio	enzyme dosage	Predictive value	Actual value	Std.Dev
BPNN	4.15	51	1:2.3	0.2334	58.61	58.14	0.80
RSM	4.55	50	1:2	0.1933	56.44	55.02	2.51

Conclusion

In this study, we performed single-factor experiments using rainbow trout skin as the raw material. The α-glucosidase inhibition rate served as the evaluation metric, while reaction temperature, reaction time, solid-liquid ratio, and enzyme concentration were the variables tested. The optimal reaction conditions for enzymatic hydrolysis are: reaction temperature of 55°C, enzymatic hydrolysis time of 4.5 h, solid-liquid ratio of 1:2, and enzyme addition amount of 0.2%. According to the factor level and response value of Box-Behnken test, RSM, BPNN model are established to optimize enzymatic hydrolysis conditions. The AGIR of the rainbow trout hydrolysate prepared under the optimal conditions of the BPNN at a concentration of 20 mg/ml is 58.14%±2.78, which is 3.09% higher than that of the RSM model. This proves that the optimization of this experiment can simultaneously improve the AGIR of the rainbow trout hydrolysate.

Funding Information

This work was supported by Foundation Grant/Award Number: 2022CXGC020414.

Authors Contributions

Yingke Chu: Conceptualization, Methodology, Software, Formal Analysis, Investigation, Data Curation, Writing - Original Draft, Visualization, Project Administration.

Yanling Dong: Conceptualization, Validation, Resources, Supervision, Funding Acquisition, Writing - Review & Editing.

Qingfeng Rong: Investigation (experimental design and execution), Formal Analysis.

Kun Yang: Methodology, Validation.

Lanlan Zhu: Conceptualization, Methodology, Software, Formal Analysis, Investigation, Data Curation, Writing - Original Draft, Visualization, Project Administration.

Ethics

This study did not involve human participants or animals. Therefore, ethical review and approval were not required.

References

Alam, F., Shafique, Z., Amjad, S. T., & Bin Asad, M. H. H. (2019). Enzymes inhibitors from natural sources with antidiabetic activity: A review. *Phytotherapy Research*, *33*(1), 41-54. https://doi.org/10.1002/ptr.6211

Bartolomei, M., Cropotova, J., Bollati, C., Kvangarsnes, K., d'Adduzio, L., Li, J., Boschin, G., & Lammi, C. (2023). Rainbow Trout (Oncorhynchus mykiss) as Source of Multifunctional Peptides with Antioxidant, ACE and DPP-IV Inhibitory Activities. *Nutrients*, *15*(4), 829. https://doi.org/10.3390/nu15040829

Bleakley, S., & Hayes, M. (2017). Algal Proteins: Extraction, Application, and Challenges Concerning Production. *Foods*, *6*(5), 33. https://doi.org/10.3390/foods6050033

Coscueta, E. R., Brassesco, M. E., & Pintado, M. (2021). Collagen-Based Bioactive Bromelain Hydrolysate from Salt-Cured Cod Skin. *Applied Sciences*, *11*(18), 8538. https://doi.org/10.3390/app11188538

de Andrade Silva, B. J., Hughes, T. K., Andrade, P. R., Ma, F., Teles, R. M. B., Shalek, A. K., Bloom, B., Pellegrini, M., & Modlin, R. L. (2020). Single-cell RNA-sequencing of leprosy skin lesions reveals a titin (TTN) expressing T cell subset associated with the progressive disease. *The Journal of Immunology*, *204*(1_Supplement), 225.36-225.36. https://doi.org/10.4049/jimmunol.204.supp.225.36

Ermias, G. A. (2021). Modeling and Optimization of Electrodialytic Desalination of Fish Sauce Using Artificial Neural. *Networks and GeneticAlgorithm*, *2759-2773*.

Fatumo, S. (2024). Including diverse populations enhances the discovery of type 2 diabetes loci. *Nature Reviews Genetics*, *25*(2), 82-82. https://doi.org/10.1038/s41576-023-00678-7

Fernández-Lucas, J., Castañeda, D., & Hormigo, D. (2017). New trends for a classical enzyme: Papain, a biotechnological success story in the food industry. *Trends in Food Science & Technology*, *68*, 91-101. https://doi.org/10.1016/j.tifs.2017.08.017

Hang, N. T., Khoa, N. M., Trang, L. T., & Phuong, N. V. (2021). Optimization of extraction of flavonoids from shallot skin using response surface methodology based on multiple linear regression and artificial neural network and evaluation of its xanthine oxidase inhibitory activity. *Journal of Food Measurement and Characterization*, *15*(3), 2173-2183. https://doi.org/10.1007/s11694-021-00811-2

Khan, M. A. B., Hashim, M. J., King, J. K., Govender, R. D., Mustafa, H., & Al Kaabi, J. (2019). Epidemiology of Type 2 Diabetes - Global Burden of Disease and Forecasted Trends. *Journal of Epidemiology and Global Health*, *10*(1), 107. https://doi.org/10.2991/jegh.k.191028.001

Kumari, S., Saini, R., Bhatnagar, A., & Mishra, A. (2024). Exploring plant-based alpha-glucosidase inhibitors: promising contenders for combatting type-2 diabetes. *Archives of Physiology and Biochemistry*, *130*(6), 694-709. https://doi.org/10.1080/13813455.2023.2262167

Kuo, C.-H., Liu, T.-A., Chen, J.-H., Chang, C.-M. J., & Shieh, C.-J. (2014). Response surface methodology and artificial neural network optimized synthesis of enzymatic 2-phenylethyl acetate in a solvent-free system. *Biocatalysis and Agricultural Biotechnology*, *3*(3), 1-6. https://doi.org/10.1016/j.bcab.2013.12.004

Lemes, A., Sala, L., Ores, J., Braga, A., Egea, M., & Fernandes, K. (2016). A Review of the Latest Advances in Encrypted Bioactive Peptides from Protein-Rich Waste. *International Journal of Molecular Sciences*, *17*(6), 950. https://doi.org/10.3390/ijms17060950

Li-na, Y., De-hong, & Chu-shu, Z. (2018). Optimization of preparation process of α-glucosidase inhibitory activity peptide with microwave assisted enzymatic hydrolysis reaction by response surface methodology. *Science and Technology of Food Industry*, *39*(4), 117-122.

Martínez-Araiza, G., Castaño-Tostado, E., Amaya-Llano, S. L., Regalado-González, C., Martínez-Vera, C., & Ozimek, L. (2012). Modeling of Enzymatic Hydrolysis of Whey Proteins. *Food and Bioprocess Technology*, *5*(6), 2596-2601. https://doi.org/10.1007/s11947-011-0624-5

Mazorra-Manzano, M. A., Ramírez-Suarez, J. C., & Yada, R. Y. (2018). Plant proteases for bioactive peptides release: A review. *Critical Reviews in Food Science and Nutrition*, *58*(13), 2147-2163. https://doi.org/10.1080/10408398.2017.1308312

Mehta, D., Shivhare, U. S., & Yadav, S. K. (2022). A statistical and neural network-assisted sustainable integrated process-based on 'zero solid waste' for the extraction of polyphenols, dietary fiber and xylooligosaccharide from de-oiled rice and corn bran. *Journal of Food Measurement and Characterization*, *16*(5), 4208-4224. https://doi.org/10.1007/s11694-022-01522-y

Meng, L., Weiwei, J., Huimin, S., & Yishan, S. (2022). Optimization of preparation technology of Antarctic krill powder peptide by response surface methodology and analysis of its inhibitory activity on α- glucosidase. *Journal of Shanghai Ocean University*, *31*(2), 564-573. https://doi.org/10.12024/jsou/20210203295

Mora, L., & Toldrá, F. (2023). Advanced enzymatic hydrolysis of food proteins for the production of bioactive peptides. *Current Opinion in Food Science*, *49*, 100973. https://doi.org/10.1016/j.cofs.2022.100973

Morales-Medina, R., Pérez-Gálvez, R., Guadix, A., & Guadix, E. M. (2016). Artificial neuronal network modeling of the enzymatic hydrolysis of horse mackerel protein using protease mixtures. *Biochemical Engineering Journal*, *105*, 364-370. https://doi.org/10.1016/j.bej.2015.10.009

Nguyen, E., Jones, O., Kim, Y. H. B., Martin-Gonzalez, F. S., & Liceaga, A. M. (2022). Correction to: Impact of microwave-assisted enzymatic hydrolysis on functional and antioxidant properties of rainbow trout Oncorhynchus mykiss by-products. *Fisheries Science*, *88*(5), 665-665. https://doi.org/10.1007/s12562-022-01614-0

O'Meara, G. M., & Munro, P. A. (1984). Effects of reaction variables on the hydrolysis of lean beef tissue by alcalase. *Meat Science*, *11*(3), 227-238. https://doi.org/10.1016/0309-1740(84)90039-1

Piyush, K., Charanjit, S. R., & Navdeep, J. (2021). Optimization of ultrasound assisted extraction of polyphenols from Meghalayan cherry fruit (Prunus nepalensis) using response surface methodology (RSM) and artificial neural network (ANN) approach. *Journal of Food Measurement and Characterization*, *15*(1), 119-133. https://doi.org/10.1007/s11694-020-00611-0

Refstie, S., Korsøen, Ø. J., Storebakken, T., Baeverfjord, G., Lein, I., & Roem, A. J. (2000). Differing nutritional responses to dietary soybean meal in rainbow trout (Oncorhynchus mykiss) and Atlantic salmon (Salmo salar). *Aquaculture*, *190*(1-2), 49-63. https://doi.org/10.1016/s0044-8486(00)00382-3

Sánchez, A., & Vázquez, A. (2017). *Bioactive peptides*. 29-46.

Wang, L., An, X., Yang, F., Xin, Z., Zhao, L., & Hu, Q. (2008). Isolation and characterisation of collagens from the skin, scale and bone of deep-sea redfish (Sebastes mentella). *Food Chemistry*, *108*(2), 616-623. https://doi.org/10.1016/j.foodchem.2007.11.017

Wu, W., He, L., Liang, Y., Yue, L., Peng, W., Jin, G., & Ma, M. (2019). Preparation process optimization of pig bone collagen peptide-calcium chelate using response surface methodology and its structural characterization and stability analysis. *Food Chemistry*, *284*, 80-89. https://doi.org/10.1016/j.foodchem.2019.01.103

Zheng, N., Chen, F., Wang, Z., & Lin, J. (2013). Modeling and Optimization of Artificial Neural Network and Response Surface Methodology in Ultra-high-Pressure Extraction of Artemisia argyi Levl. et Vant and its antifungal activity. *Food Analytical Methods*, *6*(2), 421-431. https://doi.org/10.1007/s12161-012-9439-x

Zhou, Q. L., Yang, C. G., Ren, Y. K., Ma, Q., Yang, Y. S., Wang, L. Y., & Chen, G. (2024). Histological characterization and lncRNA-mRNA integrated profiling analysis of the scales in rainbow trout (Oncorhynchus mykiss) under salinity acclimation. *Aquaculture*, *586*, 740772. https://doi.org/10.1016/j.aquaculture.2024.740772